Advanced Composite Materials
Publication details, including instructions for authors and subscription information:
http://www.tandfonline.com/loi/tacm20

Tensile strength of CFRP cross-ply laminates containing transverse cracks

Junji Noda , Tomonaga Okabe , Nobuo Takeda & Masao Shimizu

Version of record first published: 02 Apr 2012.

Adv. Composite Mater., Vol. 15, No. 1, pp. 81–93 (2006)

Also available online - www.vsppub.com

Tensile strength of CFRP cross-ply laminates containing transverse cracks

JUNJI NODA [1,*], TOMONAGA OKABE [2], NOBUO TAKEDA [3] and MASAO SHIMIZU [4]

[1] *Advanced Materials Science Research and Development Center, Kanazawa Institute of Technology, 3-1 Yatsukaho, Hakusan, Ishikawa 924-0838, Japan*
[2] *Department of Aeronautics and Space Engineering, Tohoku University, Aoba-yama 01, Aobaku, Sendai, 980-8579, Japan*
[3] *Department of Advanced Energy, Graduate School of Frontier Sciences, The University of Tokyo, 5-1-5 Kashiwanoha, Kashiwa, Chiba 277-8561, Japan*
[4] *Department of Mechanical Engineering, Keio University, 3-14-1 Hiyoshi, Kohoku-ku, Yokohama, 223-8522, Japan*

Received 20 April 2005; accepted 6 June 2005

Abstract—The effect of transverse cracks on the ultimate tensile strength (UTS) was experimentally and analytically studied for carbon fiber reinforced plastic (CFRP) cross-ply laminates. For coupon specimens of various cross-ply stacking sequences, quasi-static tensile tests were carried out and transverse cracks were observed. The experimental results showed that the measured fiber bundle strength of 0° ply was almost constant, which indicated that transverse cracks had little influence on the notch sensibility of the bundle strength. Then, we proposed a new numerical model based on the finite element method to investigate the damage extension to the fracture. This model considered the elastoplastic behavior of epoxy matrix and the fiber breakages. Using this model, we applied a Monte-Carlo method to the damage extension simulation. It was found that the plastic region at the tip of the transverse crack reduced the stress concentration due to the crack, and that the bundle strength was barely affected by transverse cracks.

Keywords: Fracture; tensile strength; transverse crack; computational simulation.

1. INTRODUCTION

Recently, carbon fiber reinforced plastic (CFRP) has been extensively used in the aerospace industry. Because of their high specific strength and stiffness, CFRP laminates are candidates as alternatives for metals such as aluminum alloys.

Edited by the JSCM.

*To whom correspondence should be addressed. E-mail: noda@neptune.kanazawa-it.ac.jp

To apply the CFRP laminates effectively to real structures, it is necessary to comprehend the mechanism of the occurrence and the propagation process of damage. Previous studies [1–9] investigated damage in laminates, especially the occurrence and the extension of transverse cracks or delamination. However, these kinds of damage occur at lower strain levels during tensile loading. Consequently, the effects of these kinds of damage on the ultimate tensile strength (UTS) have not yet been investigated quantitatively.

A simple mechanical model to explain the damage extension will enable us to apply composite laminates in various fields. Especially, the model to predict the UTS and the stress–strain relationship up to final failure may be the most attractive and useful tool to design composite structures. To predict the stress–strain relationship and the UTS of arbitrary lay-up laminates, the interaction between fiber breakages and transverse cracks should be investigated in detail.

Therefore, this study experimentally and analytically investigates the failure mechanism of various CFRP cross-ply laminates. In section 2, we measure the UTS of various cross-ply laminates and observe the damage under tensile loading. Then, section 3 proposes a numerical model to investigate the damage extension and to predict the UTS of CFRP cross-ply laminates quantitatively. Finally, section 4 discusses the effect of transverse cracks on the UTS.

2. EXPERIMENTAL

2.1. Material and experimental procedure

CFRP T800H/#3631 (Toray Industries) was used in this study. We prepared coupon specimens whose stacking sequences were unidirectional (UD) $[0]_2$ and cross-ply laminates $[0_1/90_n/01]_{n=1,2,...,6}$. Figure 1 illustrates the dimensions of these specimens. The dimensions of all specimens were 5 mm in width, 120 mm in length and 0.25–1.0 mm in thickness. GFRP tabs were glued on the specimens, and the gage length of the specimen was 50 mm. The average fiber volume fraction was 52%.

Quasi-static tensile tests were carried out at room temperature to measure the stress–strain relations and the UTS for the specimens of various stacking sequences.

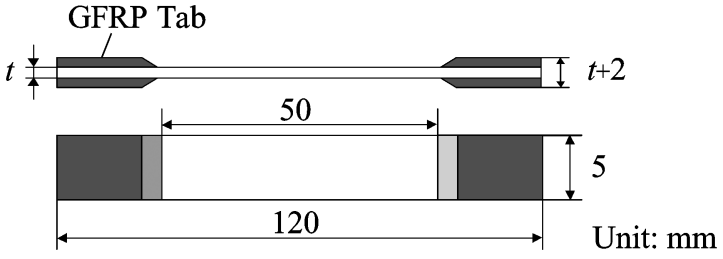

Figure 1. Dimensions of the specimens.

We observed transverse cracks by replication technique during the tests, and the polished edge of the gage section was replicated onto an acetyl cellulose film with methyl acetate as a solvent. After the tensile test, we polished the specimen ends of all specimens, and measured the thickness of 0° ply and the fiber volume fraction of 0° ply V_f^{eff}. These values were directly obtained by the photographs with an optical microscope.

2.2. Experimental results

Figure 2 shows the fiber breaks in 0° ply near the tip of a transverse crack. Delamination was not observed during the tensile tests for stacking sequences used in this study. Fiber breaks were observed near the crack tip at 1.3% strain, but the number of fiber breaks barely increased with increasing loading.

Figure 3 shows the relation between the UTS and the volume fraction of 0° ply V_0 for all the tested composite systems. Also in this figure, simply estimated strength values of cross-ply laminates from the average UTS of UD laminates $\bar{\sigma}_{UD}$ are plotted as a dashed line. Here, the estimated strength of cross-ply laminates σ_0' is given by

$$\sigma_0' = V_0 \bar{\sigma}_{UD}. \tag{1}$$

The UTS of cross-ply laminates was almost proportional to the volume fraction of 0° ply, and were well fitted to the dashed line. This fact indicates that 90° plies carry almost negligible load.

Then, we define the bundle strength as the stress shared by the fiber bundle in 0° ply at the final failure. The bundle strength σ_b is calculated by the following equation,

$$\sigma_b = \frac{\sigma_{UTS}}{V_f^{eff} V_0}, \tag{2}$$

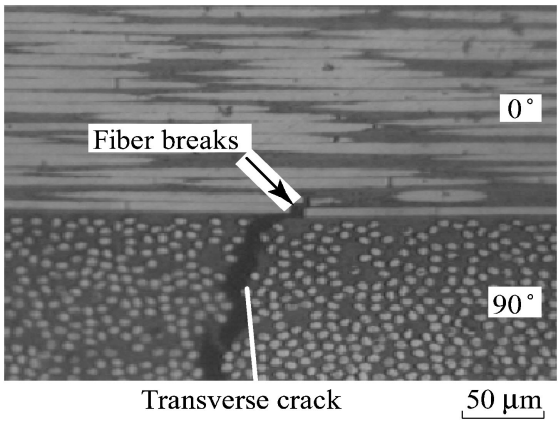

Figure 2. Photograph of the polished edge at 1.3% strain. Fiber breaks can be observed near the tip of a transverse crack.

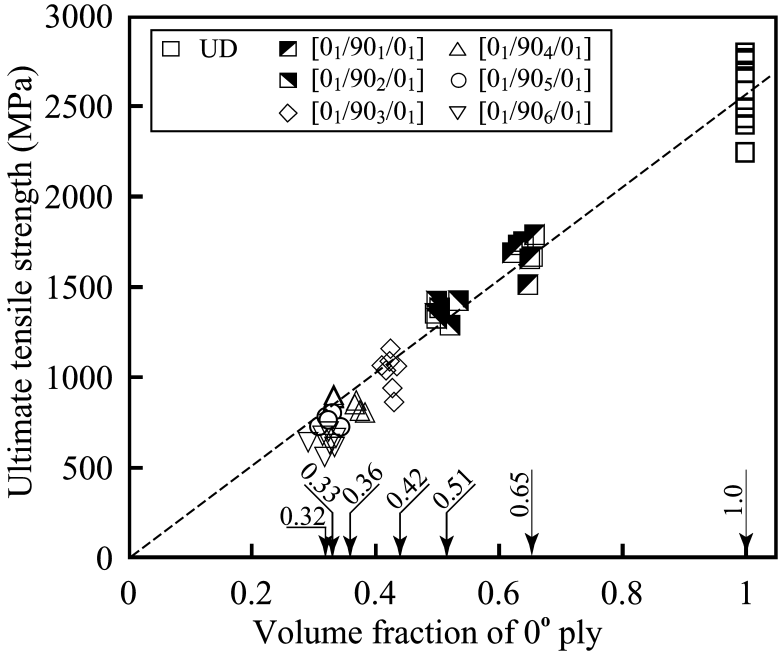

Figure 3. Relationship between the ultimate tensile strength and the volume fraction of 0° ply. The ultimate tensile strength is almost proportional to the volume fraction of 0° ply.

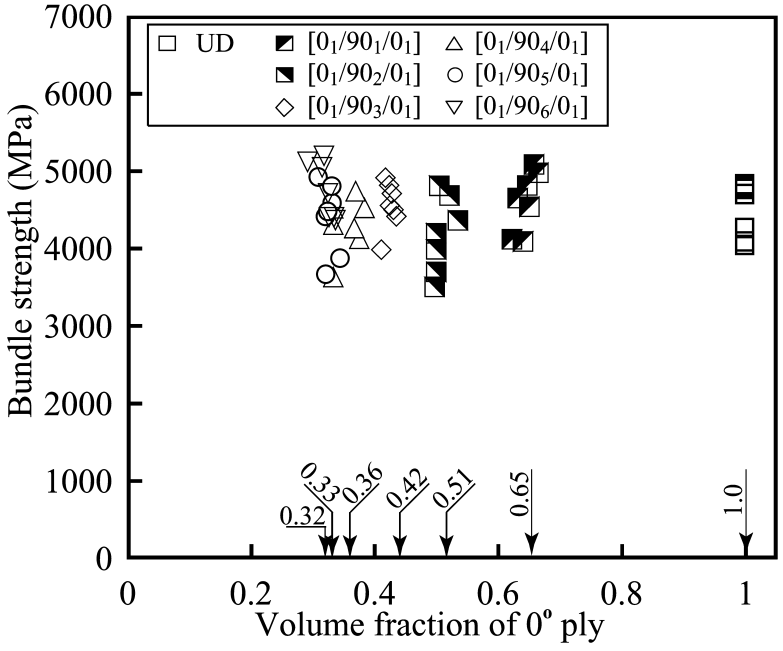

Figure 4. Relationship between the bundle strength and the volume fraction of the 0° ply. The bundle strength is almost constant independent of the volume fraction of the 0° ply.

where σ_{UTS} is the measured tensile strength. Figure 4 shows the bundle strength of each specimen in terms of the volume fraction of 0° ply. The measured bundle strength is almost constant independent of the volume fraction of 0° ply V_0. As the thickness of 90° plies increases, the length of transverse cracks along the through-thickness direction becomes longer. Then, the stress concentration at the tips of transverse cracks must increase. Consequently, the constant bundle strength shown in Fig. 4 means that the notch effects of transverse cracks on the bundle strength is negligible in these cross-ply laminates.

3. SIMULATION

We propose a detailed numerical fracture simulation (DNFS) considering various kinds of damage in the laminate. This simulation is based on finite element analysis, and the model is illustrated in Fig. 5. Because of the symmetry, a half part including a transverse crack is modeled as shown in Fig. 5a. The finite element mesh and the boundary conditions are shown in Fig. 5b. To investigate the stress recovery from the transverse crack in the 90° ply properly, we apply the fine mesh near the 0°/90° ply interface. We use 4-node isoparametric elements for the 90° ply, which have isotopic properties. As shown in Fig. 5c, elements in the 0° ply are subdivided into 2-node line elements for fibers and 4-node isoparametric elements for matrices. We assume matrix elements to be elastoplastic, with the von Mises criterion. The linear hardening law is assumed for the relationship between the equivalent stress σ_{e} and the equivalent plastic strain $\varepsilon_{\mathrm{e}}^{p}$.

$$\sigma_{\mathrm{e}} = Y + H\varepsilon_{\mathrm{e}}^{p}, \tag{3}$$

where Y is the yield stress and H is the work hardening ratio.

A transverse crack is introduced at the strain level when transverse cracks are observed in the experiment. The position of the crack is the center of the model along the tensile direction as shown in Fig. 5b. We express the crack by modifying the Young's modulus to be zero, and calculate the unloading process by assigning the nodal force at the crack interface in the reverse direction to the loading.

We assume the fibers to be linear elastic. When the axial stress in a line element exceeds the fiber strength, we define the line element as a fiber break, and apply the same unloading process with transverse cracks. We assign the strength of each fiber element based on the Weibull of Weibull concept proposed by Curtin [5]. The strength of the k-th element of the n-th fiber $\sigma_{n,k}^{s}$ is given by the Weibull distribution

$$\sigma_{n,k}^{s} = \sigma_0^n \left[\left(\frac{L_0}{\Delta L} \ln\left(\frac{1}{1-\eta_{n,k}} \right) \right) \right]^{1/\bar{\rho}}, \tag{4}$$

where L_0 is the gage length, ΔL is the length of the element, $\bar{\rho}$ is the Weibull modulus of one fiber, and $\eta_{n,k}$ is the random number within the range of (0, 1). The characteristic strength of the n-th fiber σ_0^n also follows the Weibull distribution.

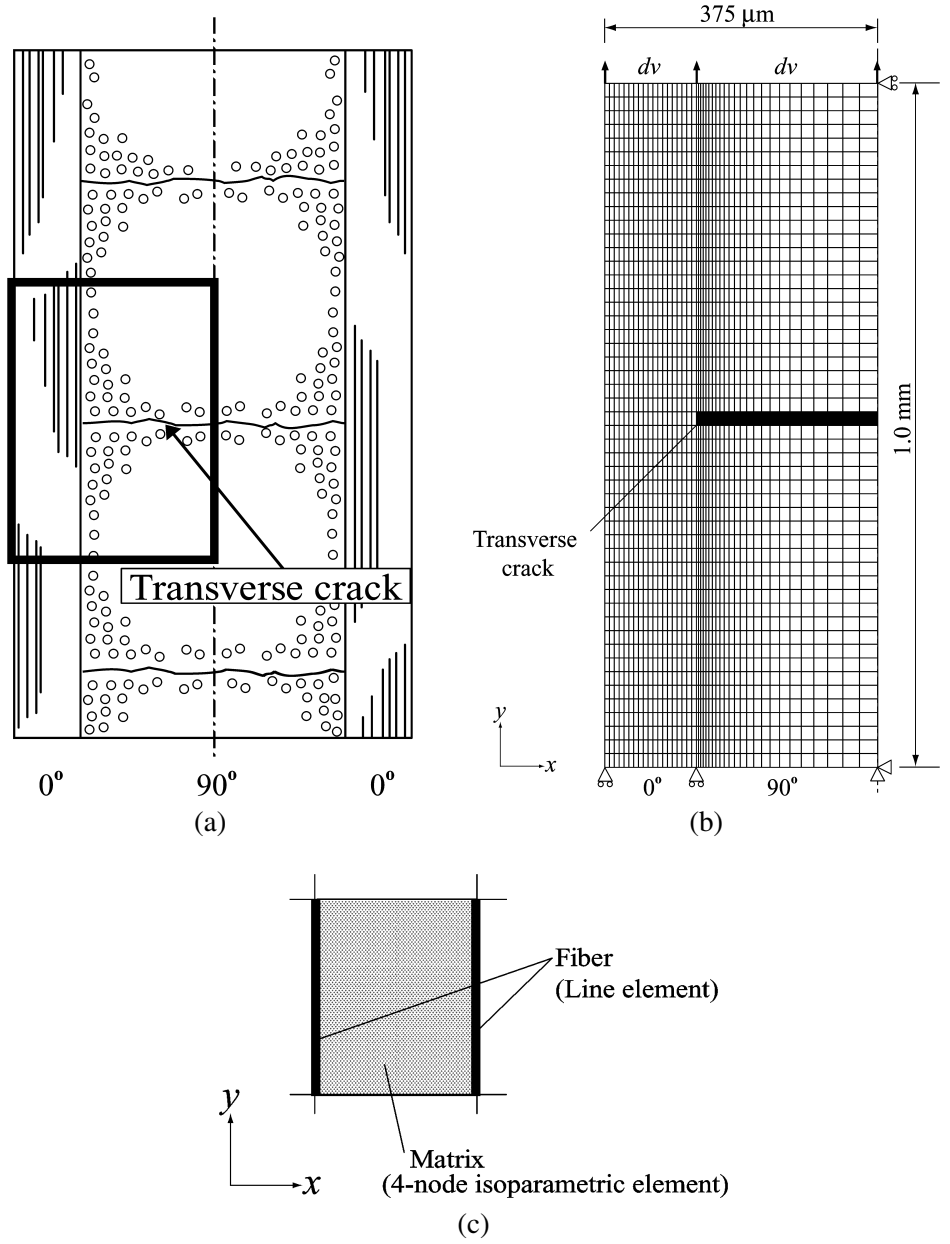

Figure 5. Finite element model used in the simulation. (a) Modeling region. (b) Finite element mesh. (c) Elements on 0° ply.

The flow chart of the simulation is shown in Fig. 6. We apply the r_{min} method proposed by Goda [10] to simulate the statistical damage process in 0° ply by judging successive damage. This method determines the incremental displacement by calculating the minimum ratio of r of the displacement for the first damage

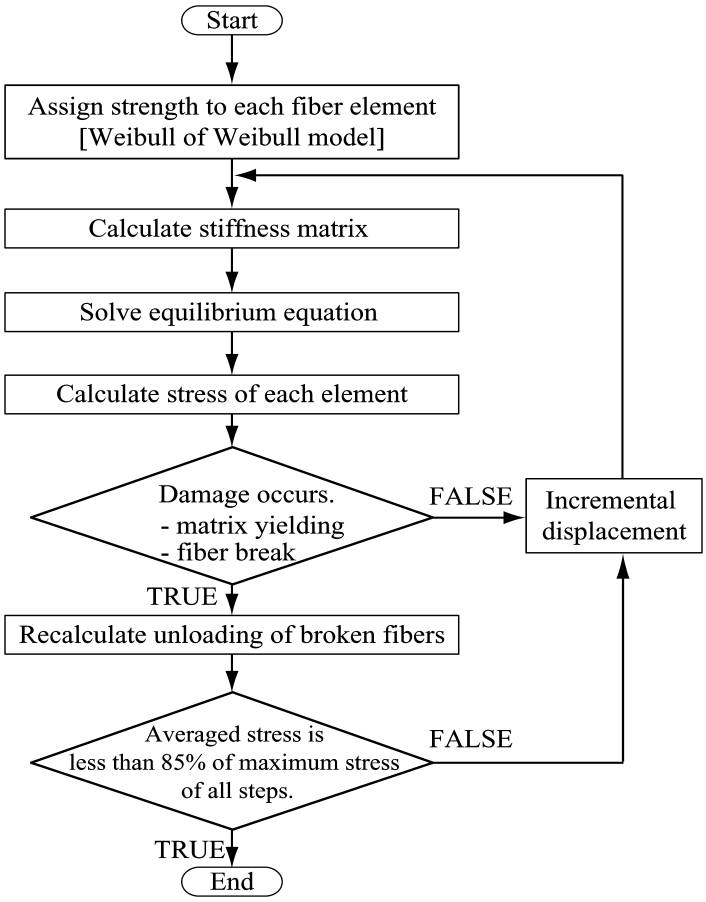

Figure 6. Flow chart of the detailed numerical fracture simulation.

occurrence with respect to each trial displacement. This enables us to judge successive damage in the simulation. This simulation calculated r for fiber breaks and yielding of matrix elements.

We assume the final failure of the model when the averaged stress decreases to 85% of the maximum stress of all the steps. The material properties used in this simulation are listed in Table 1. These values are measured ones; for fiber breaks [11], and for matrix yielding [8, 9].

Before the simulation, we investigated the effect of the mesh size of a fiber on the stress concentration around the broken fiber. Here, the model length along the fiber direction is 1 mm. The results revealed that 30 elements in a fiber were sufficient to represent the stress distribution appropriately. Therefore, we divided a fiber into 50 elements in the model. Then, the number of total nodes is 2244, and the numbers of fiber elements, matrix elements in 0° ply and 90° ply elements are 1000, 950 and 1200, respectively, for $[0_1/90_4/0_1]$ cross-ply laminates.

Table 1.
Material properties used in the simulation

Fiber in 0° ply	
Young's modulus (GPa)	294
Radius (μm)	2.5
Gage length L_0 (mm)	50
Weibull modulus $\bar{\rho}$	4
Strength based on L_0 (MPa)	3.570
Volume fraction	0.515
Matrix in 0° ply	
Yield stress (MPa)	90.8
Work hardening ratio (MPa)	75
Young's modulus (GPa)	3.165
Poisson's ratio	0.356
90° ply (transversely isotropic)	
Young's modulus (GPa)	9.57
Poisson's ratio	0.31

4. RESULTS AND DISCUSSION

4.1. Validity of the proposed model

Figure 7 compares the axial stress distribution in 90° ply by the proposed model with that by the commercial software ABAQUS. The finite element model used in ABAQUS is the same as for Fig. 5b. The stress recovery behavior by the proposed model shows good agreement with that by ABAQUS.

Furthermore, we compared the final failure estimated by the full model with that by the proposal model (1/2 model shown in Fig. 5b). We conducted the fracture simulation using the full model of $[0_1/90_4/0_1]$ laminates. Figure 8 shows the relationship between the bundle stress and the applied strain obtained by the full model. This figure also includes the bundle stresses of two 0° plies; (1) and (2). The strain at the maximum bundle stress of 0° ply (1) agrees with the strain at the maximum bundle stress in the full model. This fact indicates that the failure of the whole model occurs when the fiber bundle in a 0° ply breaks. Consequently, the proposed 1/2 model is sufficient to predict the UTS of cross-ply laminates, considering the weakest link theory for CFRP composite [5].

4.2. Simulated results

20 simulations were conducted for each stacking sequence. The comparison between simulated results and experimental results is listed in Table 2. The simulated bundle strength is plotted in Fig. 9. The simulated results are also independent of the volume fraction of 0° ply, and it is confirmed that the notch effect of the transverse cracks on the bundle strength can be negligible.

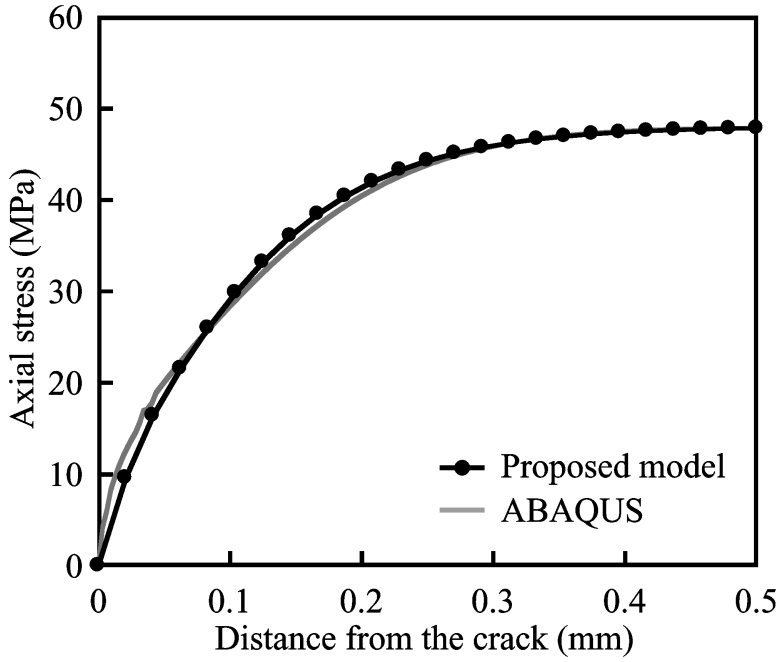

Figure 7. Comparison of axial stress distribution in the 90° ply between the proposed model and ABAQUS.

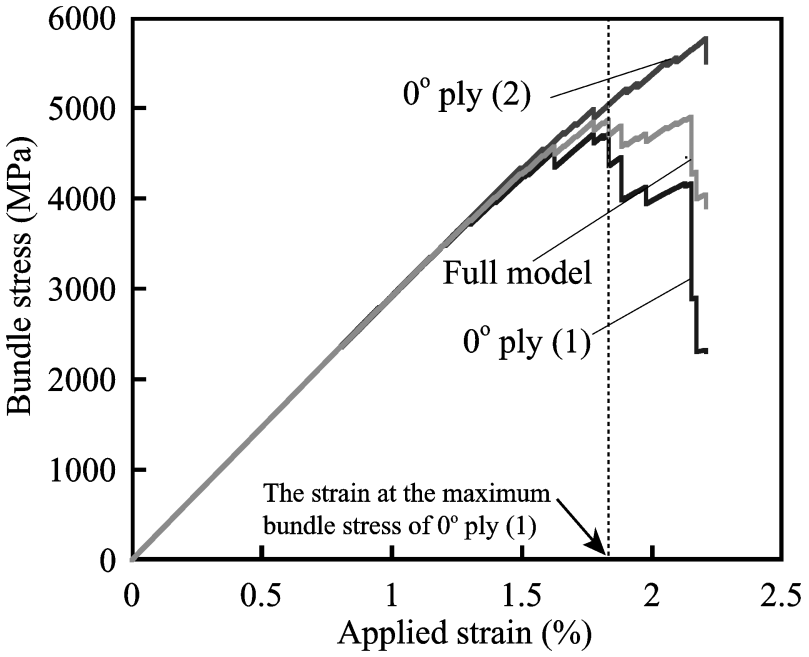

Figure 8. Relationship between the bundle stress and the applied strain using the full model of $[0_1/90_4/0_1]$ laminate. Three bundle stresses are plotted; the full model and two 0° plies.

Table 2.
Comparison of the bundle strength between the experiments and the simulations

Experiment (MPa)	Simulation (MPa)	
$[0_2]$	4033–4818	4315–5936
$[0_1/90_1/0_1]$	4085–5080	4208–5469
$[0_1/90_2/0_1]$	3499–4804	4235–6304
$[0_1/90_3/0_1]$	3979–4909	4396–5974
$[0_1/90_4/0_1]$	3626–4734	4346–6057
$[0_1/90_5/0_1]$	3649–4904	4533–5722
$[0_1/90_6/0_1]$	4360–5191	4202–5655

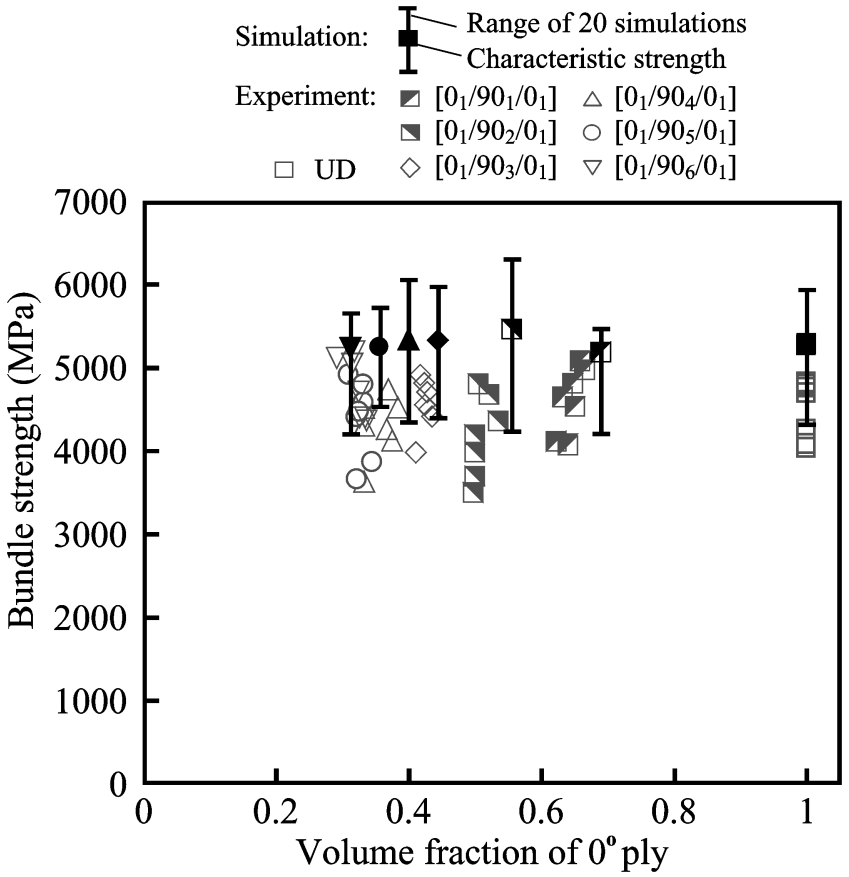

Figure 9. Simulated bundle strength of various stacking sequences. These values are also independent of the volume fraction of 0° ply.

Then, we investigate the distribution of the stress concentration on fibers during tensile loading. Figure 10 shows the typical distributions of the stress concentration factor (SCF) of fiber elements. The value of SCF is the tensile stress of each fiber

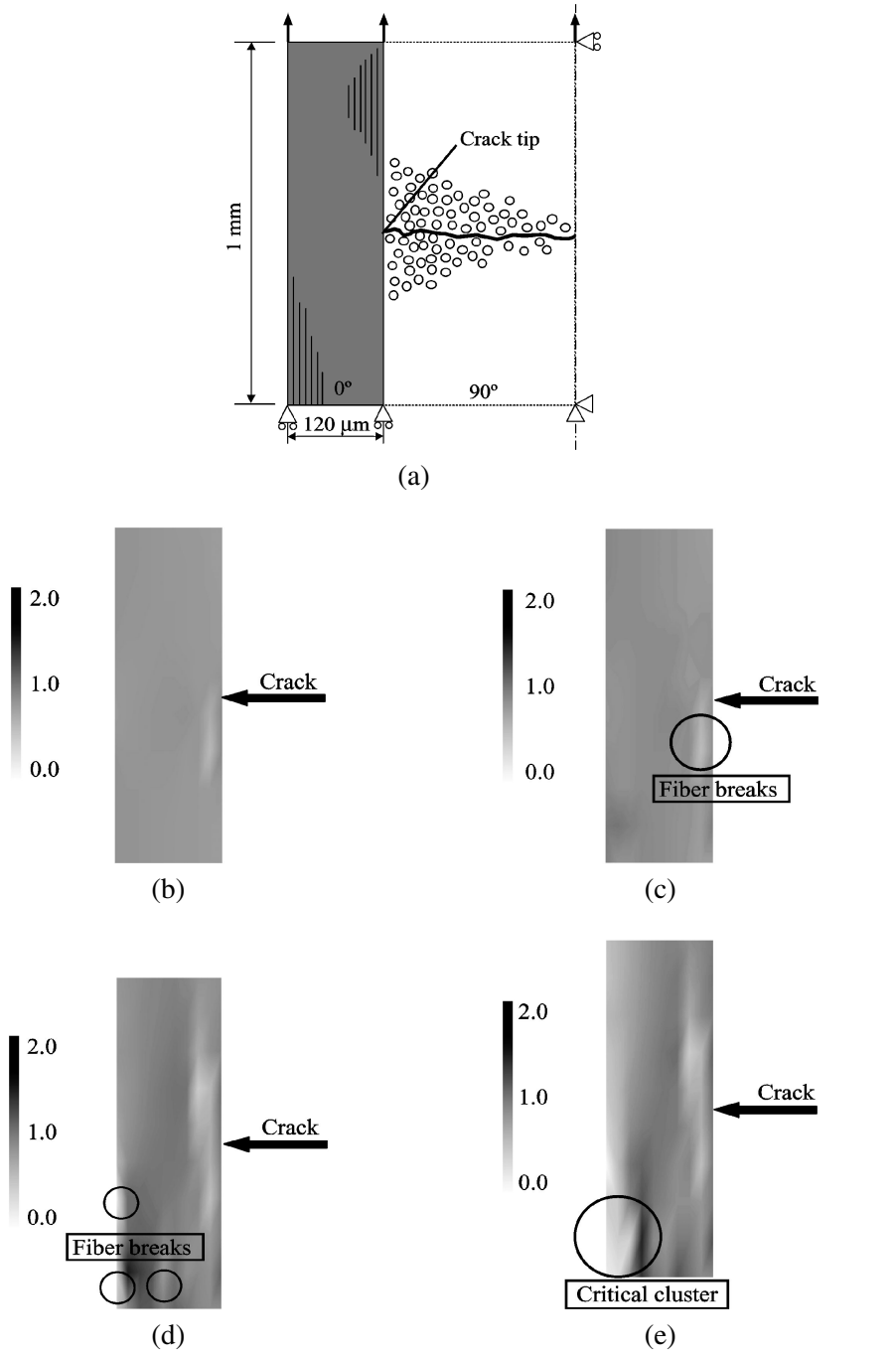

Figure 10. Typical distributions of the stress concentration factor of fiber elements in 0° ply. The critical cluster extends far from the crack tip. (a) Schematic of the reference plane (gray zone). (b) $\varepsilon = 1.23\%$. (c) $\varepsilon = 1.56\%$. (d) $\varepsilon = 2.10\%$. (e) Final failure.

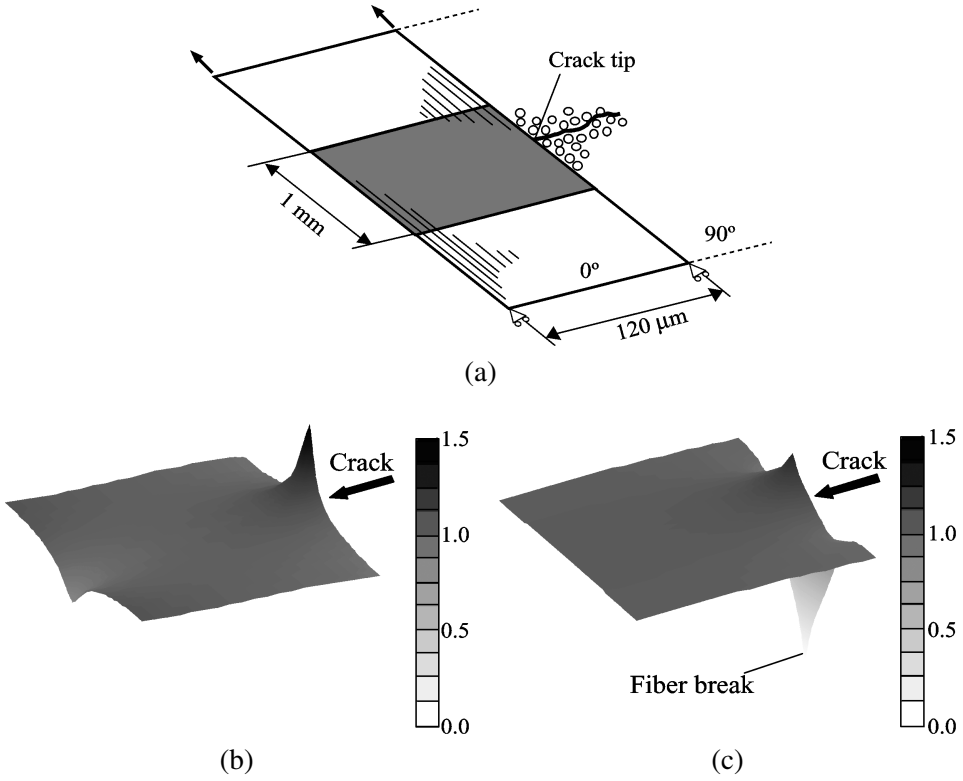

Figure 11. Change in the distribution of the stress concentration due to the fiber break. The maximum SCF reduces after the fiber break because of the plastic behavior of the matrix. (a) Schematic of the reference plane (gray zone). (b) Before fiber break. (c) After fiber break.

element normalized by the bundle stress. Although the first fiber break occurs at the tip of the transverse crack (Fig. 10b, c), fibers far from the tip of the crack break at the higher strain level (Fig. 10d). Then, the critical cluster extends far from the tip of the transverse crack as shown in Fig. 10e.

Finally, we investigate the factor of the occurrence of the critical cluster far from the crack tip. Figure 11 shows the SCF maps before and after the fiber break, respectively. It is found that the maximum value of SCF at the crack tip is significantly reduced after the fiber break, although the stress concentrated region is enlarged. This phenomenon occurs because of the plastic behavior of the matrix near the crack tip. These simulated results can explain the results shown in Fig. 9; the bundle strength of 0° ply becomes independent of transverse cracks. Consequently, plastic behavior of the matrix reduces the stress concentrations due to transverse cracks, and the final failure of the cross-ply laminate is less sensitive to transverse cracks.

5. CONCLUSIONS

This paper studied the effect of transverse cracks on the ultimate tensile strength in CFRP cross-ply laminates through experiments and numerical simulations. The major results of this study are summarized below.

(1) The bundle strength measured in the experiment was independent of the thickness of the 90° ply, although the stress concentration at the tips of transverse cracks increased. This means that the notch sensitivity of the transverse cracks on the bundle strength is negligible.

(2) The authors proposed a detailed numerical fracture simulation based on a finite element method to investigate the interaction between fiber breaks and transverse cracks.

(3) The simulated results showed that plastic behavior of the matrix reduced the stress concentration near the tips of transverse cracks. Then, the bundle strength of 0° ply became independent of transverse cracks. Finally, the final failure of the cross-ply laminate was less sensitive to transverse cracks.

REFERENCES

1. A. S. D. Wang and F. W. Crossman, Initiation and growth of transverse cracks and edge delamination in composite laminates, Part 1. An energy method, *J. Compos. Mater.* **14**, 71–87 (1980).
2. N. Takeda and S. Ogihara, *In situ* observation and probabilistic prediction of microscopic failure processes in CFRP cross-ply laminates, *Compos. Sci. Technol.* **52**, 183–195 (1994).
3. N. Takeda and S. Ogihara, Initiation and growth of delamination from the tips of transverse cracks in CFRP cross-ply laminates, *Compos. Sci. Technol.* **52**, 309–318 (1994).
4. S. Ogihara, N. Takeda and A. Kobayashi, Experimental characterization of microscopic failure process under quasi-static tension in interleaved and toughness-improved CFRP cross-ply laminates, *Compos. Sci. Technol.* **57**, 267–275 (1997).
5. W. A. Curtin, Tensile strength of fiber-reinforced composites: III. Beyond the traditional Weibull model for fiber strengths, *J. Compos. Mater.* **34**, 1301–1332 (2000).
6. T. Okabe, N. Takeda, Y. Kamoshida, M. Shimizu and W. A. Curtin, A 3D shearlag model considering micro-damage and statistical strength prediction of unidirectional fiber-reinforced composites, *Compos. Sci. Technol.* **61**, 1773–1787 (2001).
7. F. M. Zhao, T. Okabe and N. Takeda, The estimation of statistical fiber strength by fragmentation tests of single-fiber composites, *Compos. Sci. Technol.* **60**, 1965–1974 (2000).
8. T. Okabe and N. Takeda, Estimation of strength distribution for a fiber embedded in a single-fiber composite: experiments and statistical simulation based on the elasto-plastic shear-lag approach, *Compos. Sci. Technol.* **61**, 1789–1800 (2001).
9. T. Okabe and N. Takeda, Elastoplastic shear-lag analysis of single-fiber composites and strength prediction of unidirectional multi-fiber composites, *Composites Part A* **33**, 1327–1335 (2002).
10. K. Goda, The role of interfacial debonding in increasing the strength and reliability of unidirectional fibrous composites, *Compos. Sci. Technol.* **59**, 1871–1879 (1999).
11. T. Okabe and N. Takeda, Size effect on tensile strength of unidirectional CFRP composites — experiment and simulation, *Compos. Sci. Technol.* **62**, 2053–2064 (2002).